Finite Element Analysis of Silicone Rubber Spacers Used in Automotive Engine Control Modules

Fereydoon Dadkhah
Arlene Zahiri
Delphi Electronics and Safety
Kokomo, IN

Abstract

Silicone Rubber Spacers in the shape of truncated cones are used in automotive electronic applications to ensure thermal or electrical contact between different components. In one such application, the “cones” are used in Engine Control Modules (ECM) to press flip chip Integrated Circuits (IC) against metal heat sinks to provide a conduction heat transfer path. The spacer size and height has to be specified in order to exert sufficient pressure on the face of the flip chips. The silicone rubber material exhibits a nonlinear force deflection curve and assuming linear behavior would lead to designing incorrectly sized spacers which would either not provide enough pressure for efficient heat transfer or excessive force which may cause damage to the system.

This paper describes an effort undertaken at Delphi Electronics and Safety to characterize the silicone rubber material and simulate its behavior using finite element analysis and the Mooney Rivlin material model. Cubic and Cylindrical spacers were built and tested to establish force-deflection and stress-strain curves for the material and to calculate the Mooney Rivlin constants. Since the material is used in compression only, only uniaxial compression tests were performed. The finite element models using the Mooney Rivlin constants were validated by reproducing the measured data for the cylindrical and cubic samples before they were used to model truncated cone and pyramid shape spacers.

Introduction

Engine control modules house the electronics that monitor and control automobile engine operation. The housing of an ECM is designed to suit the mounting location of the ECM and is typically made of cast Aluminum or Steel for units that are to be mounted in the engine compartment. The housing has the task of protecting sensitive electronics from the very harsh environment of the engine compartment. This environment includes vibration, heat, and corrosive materials which have to be kept away from the ICs housed in the ECM. In addition, the operation of the electronics circuitry inside the ECM generates a large amount of heat which has to be removed. Failure to adequately cool the ECM electronics can quickly lead to overheating and failure.

The patented system shown in Figure 1 uses pedestals built into the housing to conduct heat away from the ICs. The pedestals are cast in various shapes and heights to suit a particular IC. The spacers are mounted on an Aluminum cover which when assembled, causes the ICs to be pressed against the heat sinks. Once the unit is assembled, the ICs must not separate from the pedestal surface, not only because the loss of the heat transfer path, but also because of vibration and shock issues. Insufficient spacer force would cause the ICs to strike the pedestal surface and very quickly lead to failure. On the other hand the force exerted by the spacer cannot be arbitrarily set high due to cover and PCB design considerations.

Designers were previously forced to estimate elastomer force by using linear calculations, which can lead to very large errors when dealing with hyperelastic materials. It was discovered that up to approximately 20% strain, linear calculations predicted the spacer force fairly accurately, however in some cases, the force exerted on the IC by the spacer at this level of compression is insufficient. This is particularly true in the case of larger ICs and rectangular ICs with very high aspect ratios between length and width.

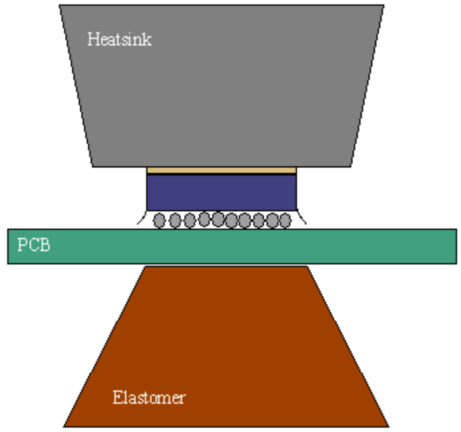

Figure 1. Cross-sectional view

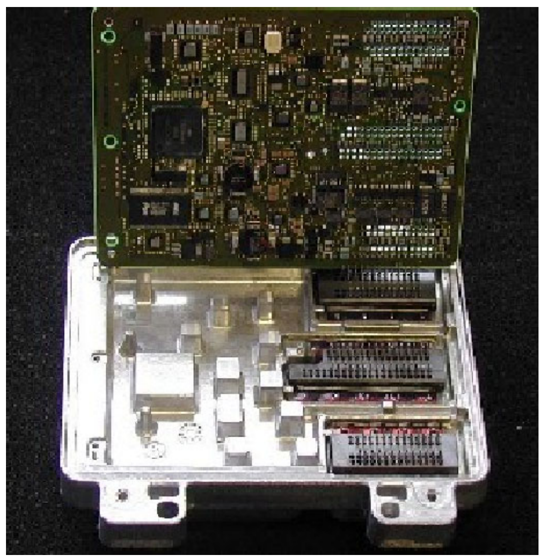

Figure 2. Housing and circuit board assembly

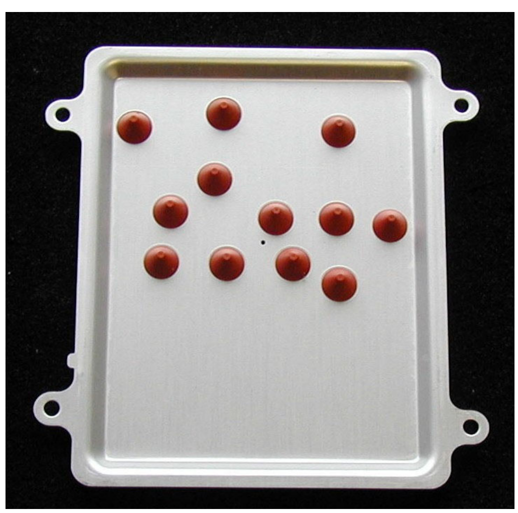

Figure 3. Cover and spacers

Methodology

This activity was carried out in two phases as described below.

The goal of the first phase was to characterize the elastomer material and develop the FEA tool. The material was characterized by building cylindrical and cubic shaped samples (Figure 4) and compressing them in an Instron machine. The force-deflection curves obtained in this way were used in the rest of the project. The 5-term Mooney-Rivlin material model was chosen for use in the FEA models. Equation 1 [1] shows the 5 parameter Mooney-Rivlin model which expresses the strain energy potential function W in terms strain invariants I and the material constants C and d.

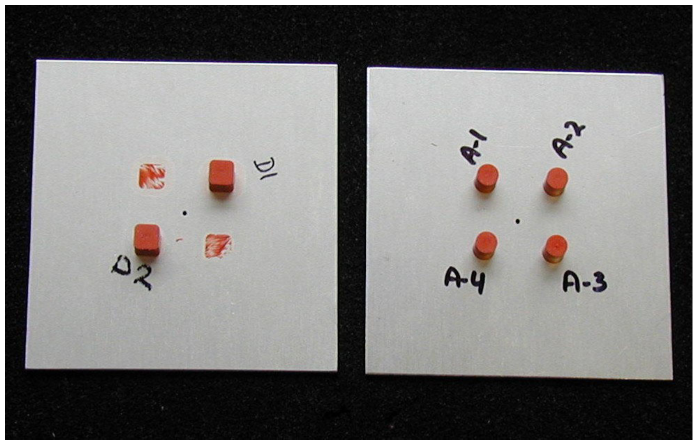

Figure 4.

Equation 1

$$W = c_{10}(\bar{I}_1 - 3) + c_{01}(\bar{I}_2 - 3) + c_{20}(\bar{I}_1 - 3)^2$$

$$+ c_{11}(\bar{I}_1 - 3)(\bar{I}_2 - 3) + c_{02}(\bar{I}_1 - 3)^2 + \frac{1}{d}(J - 1)^2$$

where:

c_{10}, c_{01}, c_{20}, c_{11}, c_{02}, d = material constants

A complete explanation of equation 1 and constants please refer to the ANSYS Theory Reference Manual [1]. Although the total strain experienced by the spacers is almost always below 50%, and conventional wisdom is to use a two-term model in that range, this rule applies to elastomers in tension. In order to accurately model hyperelastic materials in this range of compression, a 5-term model is necessary.

The constants for the M.R. model were originally determined using the ANSYS 5.7 *MOONEY macro and later using the curve fitting capabilities of the TBFT command in ANSYS 7.0. The command and the macro take engineering stress-strain data as input and produce the constants for the specified curve-fit using the least-squares fit.

Once the constants were established, two FEA models were developed and validated by reproducing the measured data with very good accuracy. An axisymmetric model was developed to verify the data collected from the cylindrical samples and a 3-dimensional model was used for the cubic samples taking advantage of 1/4 symmetry.

The goal of the second phase was to predict force deflection curves for new spacers as well as establish curves for spacers already in use. Currently, two spacer forms are used in Engine Control Modules; truncated cones (type 1), and a hexahedron shaped spacer which is referred to as a *pyramid* (type 2), Figure

5. In this phase also two models were developed to take advantage of the symmetry present in the spacer shapes.

As a further verification of the models, data that had been previously collected for the type 2 spacers were used to make certain that the constants developed in phase 1 could be used to analyze type 1 and 2 spacers. Once this was established, the models were used to predict force-deflection curves for spacers of different sizes.

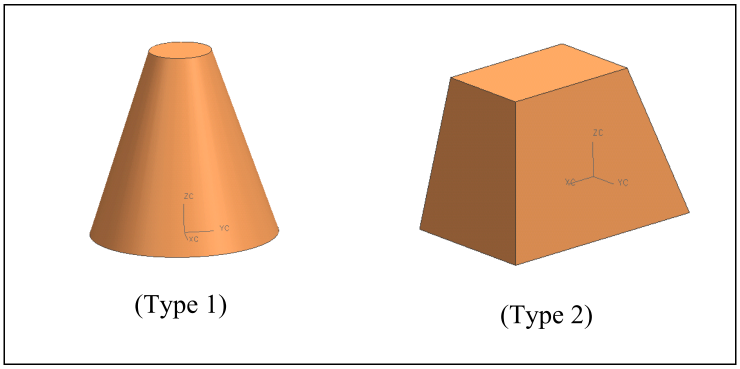

Figure 5.

Experimental Data

The ANSYS MOONEY macro and TBFT command use engineering stress-strain data and calculate the required constants for the Mooney-Rivlin formulation. For hyperelastic materials, six deformation states are used to generate the data necessary for the curve fits. These are uniaxial tension, uniaxial compression, equibiaxial tension, equibiaxial compression, planer tension, and planer compression. The deformation states can be reduced to three since it can be shown that three of the modes are equivalent with the remaining three. In the case of this analysis, only Uniaxial compression was used since the spacers are only used in compression [6][1]. It important to note that the constants calculated as a result of these tests can only be used for analysis of spacers in compression.

In order to generate the pure state of strain required as nearly as possible, spacers in the shape of cylinders and cubes were made and tested. The specimens' constant cross-sectional geometry allowed for easy calculation of the compressive stress in the samples. Four cubes and six cylinders were compressed up to 4mm, which constitutes a 50% strain. All the samples were tested under similar conditions and force v. displacement data was collected for each sample.

Figures 6 and 7 show the force-displacement curves obtained for the cylindrical and cubic samples respectively.

Load rate and ambient temperature, two of the most important factors in testing elastomers were kept the same for all samples, therefore the larger variation observed in figure 6 is assumed to be due to dimensional variation in the cubes. Another important factor in compressive tests of elastomers is friction between the instrument and the sample. Ideally, friction should be zero, so that the sample is put into a purely compressive state. The ability to accurately reproduce the measured force-deflection curves indicates that the combined affect of these uncontrolled factors is not significant for the purposes of this study.

Material properties of elastomer materials are known to change significantly after repeated loading sequences to the same strain level [5]. In other words the stress-strain curve observed during the first loading cycle changes significantly, if the specimen is unloaded and reloaded to the same strain level. However, in the present application, the loading cycle occurs only once during assembly. Once assembled, the units are never disassembled except for failure analysis purposes.

The assembled units are however, subject to vibration both during validation testing and normal use. In both circumstances, the spacers experience a dynamic strain superimposed on a mean strain level. This phenomenon and its variation with temperature is not addressed in the present effort and will be the subject of a future study.

Friction between the spacers and the PCB is another factor which is difficult to quantify. Experimenting with the friction factor used in the cylindrical model showed a variation of 8% in the maximum force when the value was changed from 0 to 0.95. Unfortunately, the exact value of friction factor will depend on the site of contact between the spacer and the PCB since the boards are typically double sided, i.e., components are mounted on both sides and the spacers may contact the board on a surface dotted with leads protruding from the opposite side which would increase friction considerably. Fortunately, the effect of friction on the actual spacers (types 1 and 2) is minimized because the shape of the spacers helps to prevent spreading of the spacer surface at point of contact with the circuit board. This phenomenon can be seen in Figure 11.

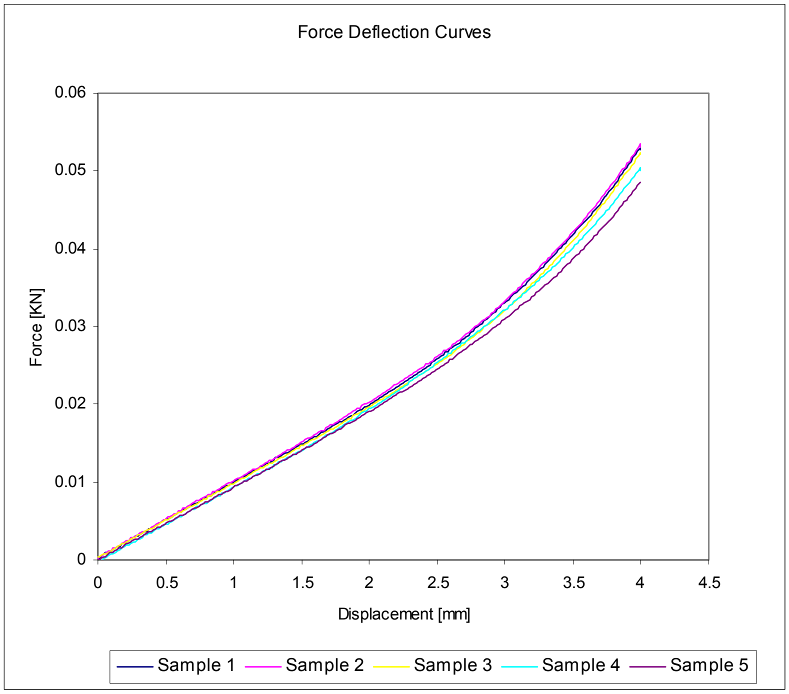

Figure 6. Cylindrical sample results

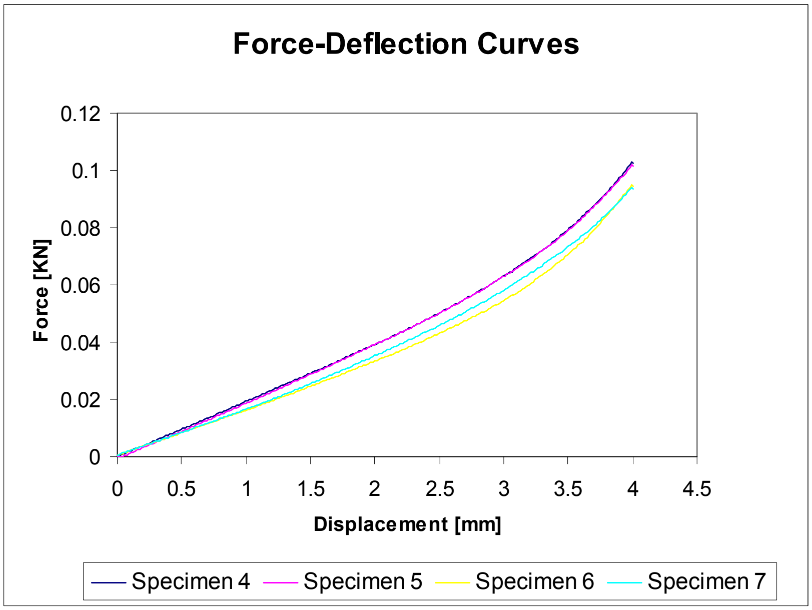

Figure 7. Cubic sample results

For both sample geometries, a representative data set was used to calculate the stress-strain curve and the Mooney Rivlin constants. Ultimately, the Mooney-Rivlin constants obtained by using the cylindrical samples were used since they resulted in better correlation with measurements.

Finite Element Models

In order to validate the experimental data and the models, finite element analyses of the cylindrical, and cubic samples were performed. The goal of these analyses was to reproduce the measurements taken in the lab. Since the data collected from the cylindrical and cubic samples were used to calculate the Mooney-Rivlin constants, it was crucial that the FEA models be able to reproduce this data.

Figure 8 shows the deformed shape of the cylindrical sample model at 3 mm, and Figure 9 shows the comparison of FEA and measurement data.

Validity of the simulations was further established when FEA results for Type 2 spacers were compared to measured data as shown in Figure 10. Figure 11 shows the deformed shape of the type 2 spacer at maximum compression.

A summary of the FEA models for both 2-D axisymmetric models and the three-dimensional models is given in table 1. The Hyper74 and Hyper58 elements proved very robust for this application and converged relatively quickly.

In both 3-D and axisymmetric models rounded corners were needed for stability and quick convergence, therefore, a 0.25mm radius fillet was added to the models to avoid convergence problems. This is in line with the actual geometry since the spacers do have rounded corners.

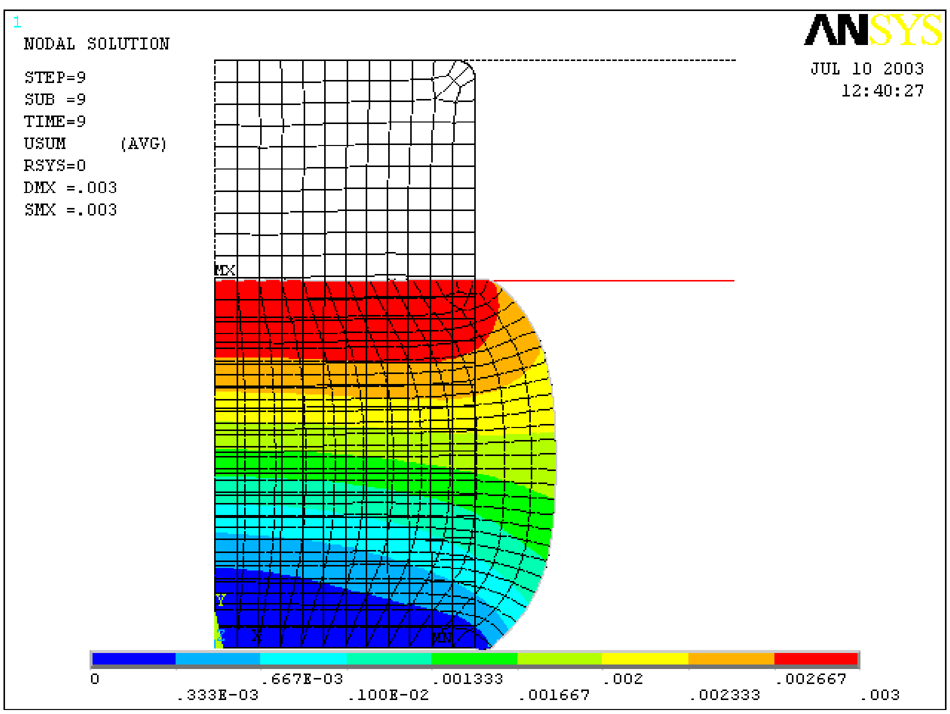

Figure 8. Deformation of the cylindrical sample

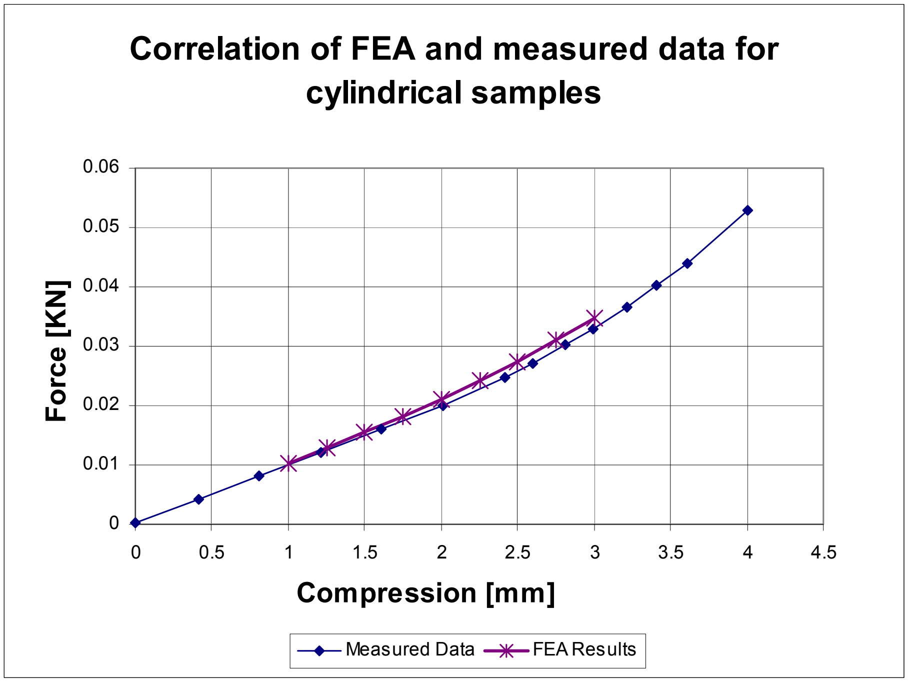

Figure 9. Comparison of results for cylindrical samples

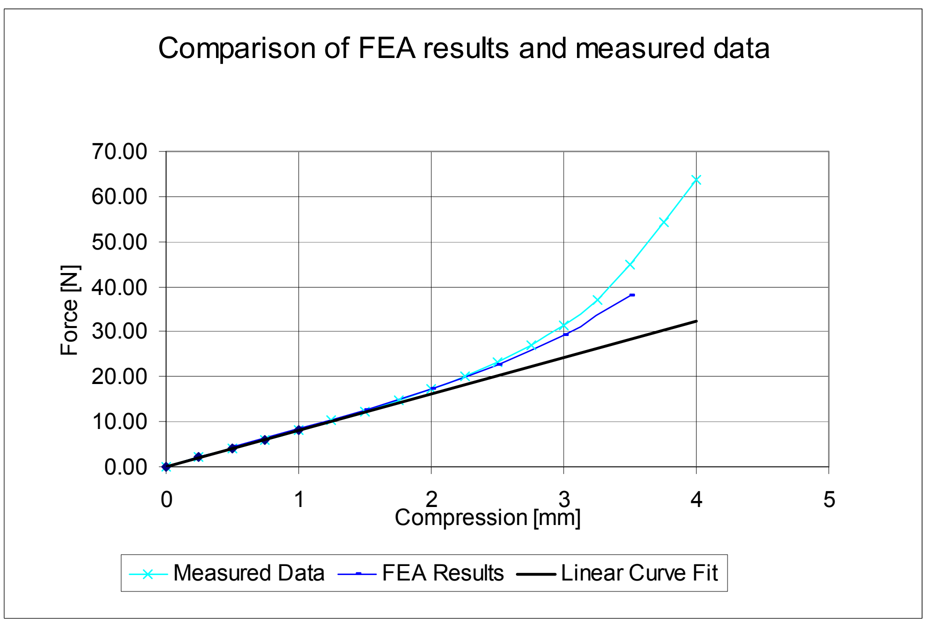

Figure 10. Comparison of results for Type 2 spacers

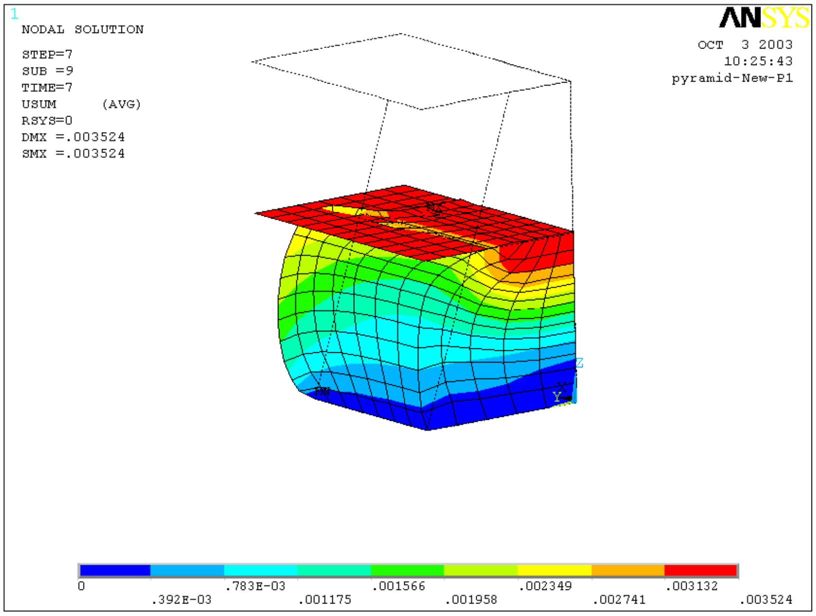

Figure 11. Deformed shape of type 2 spacer

Table 1

	Element Type	Contact Element	Target Element
Axisymmetric Models	Hyper74	172	169
3-D Models	Hyper58	174	170

The results of the FEA model for type 1 spacers were used to calculate pressure exerted on the ICs of an ECM as a result of compression of the spacers. The normalized results for three of the ICs are shown in table 2. These results when compared to shaker results obtained previously indicated that the IC with the lowest calculated pressure (#3) consistently suffered damage. This indicates the spacer exerted insufficient pressure to keep the IC in contact with the pedestal during vibration, therefore allowing the IC to repeatedly strike the pedestal surface.

Table 2

IC	Normalized Pressure
1	3.04
2	2.25
3	1
4	2.32

Vertical Application

Due to the simplicity of the various geometries involved, developing an automated tool to calculate force-deflection data for spacers was a natural development. APDL (ANSYS Parametric Design Language) scripts that were developed to model cylindrical and cubic spacers were modified and enhanced to analyze Type 1 and Type 2 spacers as well.

Post-processing scripts were also developed to collect the information that is of interest to a product engineer and to present this information in tabular form.

Once the scripts were tested, a C++ Graphical User Interface was developed to collect the dimensional data from a product engineer (without FEA experience) and to execute the model. Figure 12 shows the GUI. The results of the analysis are then collected in one ASCII file, which is shown in Figure 13.

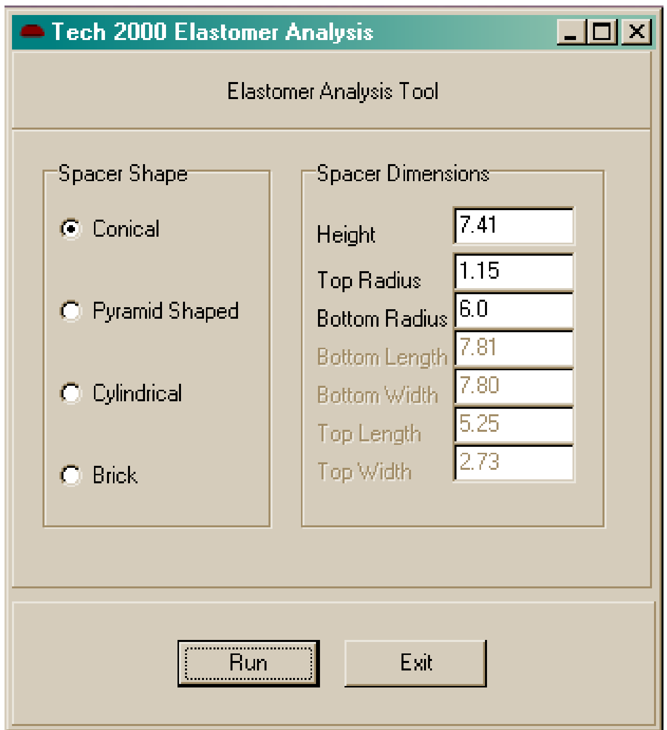

Figure 12.

```
 Job Name = cone
 Title = K-Elastoastomer mer AnalAnalysis
 top radius =  0.1150E-02 bottom radius =  0.6000E-02 height =  0.7410E-02
Step  Compression [mm]  Radius[m]   Area[m2]     Force[N]    Pressure[Pa]
 1.     0.2500         0.1150E-02   0.4155E-05    1.273        1107.
 2.     0.5000         0.1302E-02   0.5322E-05    2.534        1947.
 3.     0.7500         0.1302E-02   0.5322E-05    3.777        2902.
 4.      1.000         0.1453E-02   0.6634E-05    5.080        3496.
 5.      1.250         0.1605E-02   0.8090E-05    6.522        4064.
 6.      1.500         0.1756E-02   0.9690E-05    8.128        4628.
 7.      1.750         0.1908E-02   0.1143E-04    9.991        5237.
 8.      2.000         0.2059E-02   0.1332E-04    12.15        5899.
 9.      2.250         0.2211E-02   0.1536E-04    14.68        6638.
10.      2.500         0.2363E-02   0.1753E-04    17.75        7513.
11.      2.750         0.2514E-02   0.1986E-04    21.51        8555.
12.      3.000         0.2817E-02   0.2493E-04    26.30        9337.
```

Figure 13. Sample output from automated analysis

Conclusions

Silicone-Rubber spacers used in automotive engine control modules were successfully characterized and finite element models using the Mooney-Rivlin material model have been developed to accurately predict force deflection characteristics of the spacers. Additionally, an automated tool has been developed which only requires the user to input geometric information in order to calculate the force deflection of a spacer.

Close correlation with measurement indicates that the models can be used to predict static behavior of the spacers with confidence. However, gathering and using additional data regarding the elastomer material including the following can further improve the accuracy of the models.

- Temperature at assembly
- Load rate during assembly
- Degradation due to permanent set

References

1 - Hyperelasticity. ANSYS 7.1 Documentation, ANSYS Inc. Theory Reference Manual. Section 4.5.

2 - Electronics Materials Handbook. ASM International, Merrill L. Minges Technical Chairman. 1989.

3 - Richard A. Flinn, Paul K. Trojan: Engineering Materials and Their Applications. Houghton Mifflin Company, 1981.

4 - James W. Dally: Packaging of Electronic Systems. McGraw-Hill Inc. 1990.

5 - Kurt Miller: Experimental Loading Conditions Used to Implement Hyperelastic and Plastic Material Models. Axel Products Inc.

6 - Kurt Miller: Testing Elastomers for ANSYS. Axel Products Inc.